Two Dimensional Counterpropagating Spatial Solitons in Photorefractive Crystals

M. Petrović,[1] D. Jović,[1] M. Belić,[1,2] J. Schröder,[3] Ph. Jander,[3] and C. Denz[3]

[1]Institute of Physics, Post Office Box 57, 11001 Belgrade, Serbia
[2]Texas A&M University at Qatar, Post Office Box 5825, Doha, Qatar
[3]Institute of Applied Physics, Westfälische Wilhelms-Universität Münster Corrensstr., 2/4, D-48149 Münster, Germany

(Received 16 September 2004; published 25 July 2005)

We demonstrate experimentally the existence of two transverse-dimensional counterpropagating (CP) incoherent spatial solitons in a $5 \times 5 \times 23$ mm SBN:60Ce photorefractive crystal and investigate their dynamical behavior. We carry out numerical simulations that confirm our experimental findings. Substantially different behavior from the copropagating incoherent solitons is found. A symmetry breaking transition from stable overlapping CP solitons to unstable transversely displaced CP solitons is observed. We perform linear stability analysis that predicts the threshold for the splitup transition, in qualitative agreement with numerical simulations and experimental results.

DOI: 10.1103/PhysRevLett.95.053901 PACS numbers: 42.65.Tg, 42.65.Sf

Optical spatial solitons have become one of the latest paradigms in physics [1]. Important for applicative potential in all-optical information processing, they are generated in a variety of media, by a variety of nonlinear mechanisms [2]. A common thread to all mechanisms is the self-focusing effect, produced by light-induced changes in the medium's index of refraction. In photorefractive (PR) crystals self-focusing is achieved through the formation of space charge field, caused by the photo-induced redistribution of charges in the crystal, which in turn modifies the refractive index via the linear Pockels effect.

The formation and interactions of incoherent spatial screening solitons in two transverse dimensions (2D) have been studied mostly in the copropagation geometry. Diverse phenomena have been observed, such as soliton spiraling [3], fusion [4], filamentation [5], and modulational instabilities [6]. However, overlapping copropagating solitons are found to be stable. The "dynamics" of all these phenomena have been considered with respect to z, the propagation direction; no real time has been involved. Temporal development was followed in a few publications in 1D, displaying an approach to steady state [7]. The only publication treating dynamical effects in 2D, that we are aware of, is our own [8]. Counterpropagating (CP) solitons were investigated in a few publications [9–12], also in 1D. They were studied theoretically in Kerr and local PR media, in the steady state. In addition, Refs. [11,12] contain an experimental observation of stable CP solitons in an SBN60 crystal, formed by coherent fields, in the form of narrow stripes.

Here we present the first experimental evidence of 2D CP incoherent vector solitons in a similar crystal, display the transverse splitup instability of such solitons when the propagation distance and the coupling constant are varied, and observe dynamical instabilities at higher values of these parameters. We follow instabilities in time, as well as in z. We find that the behavior of CP solitons is essentially different from the copropagating solitons, which show no sign of such instabilities. Using linear stability analysis (LSA), we attempt to explain the splitup instability as a first-order phase transition, caused by spontaneous symmetry breaking [13], and determine the threshold curve. We perform numerical simulations of CP beams in PR media with time-dependent nonlinearity, to qualitatively confirm experimental findings and stability analysis.

The study of CP beams is performed in the experimental setup of Fig. 1. Laser beam derived from a frequency-doubled Nd:YAG laser emitting at 532 nm is split and focused onto the opposite faces of a photorefractive SBN60:Ce crystal ($5 \times 5 \times 23$ mm), along one line. The beam components are made incoherent in the medium by reflecting one component off the vibrating piezo mirror (PM). The c axis of the crystal is placed along one of the 5 mm edges, so that by rotating the crystal both the 23 mm axis and the other 5 mm axis can be utilized as propagation directions of the beams. To exploit the dominant electro-optic component $r_{33} \approx 200$ pm/V of our SBN sample, the incident laser beams are linearly polarized parallel to the c axis, perpendicular to the propagation direction. A dc electric field, necessary for the screening effect, is applied across the crystal along the c axis, and the crystal is illuminated by uniform white light, to create artificial

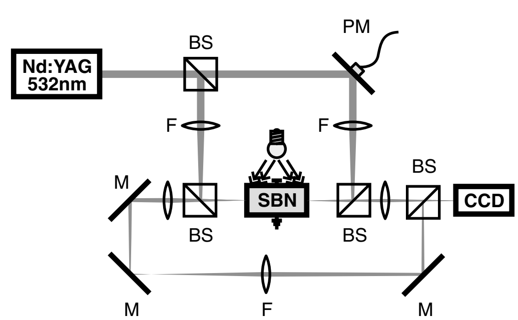

FIG. 1. Experimental setup for the investigation of CP solitons.

dark conductivity. Both input and output faces of the crystal are monitored by CCD cameras.

Stable CP solitons are readily observed over the 5 mm propagation distance, with an applied field of 1.3 kV/cm and the initial beam peak intensity of about twice the background intensity. Incoherent Gaussian beams of 20 μm FWHM are launched head-on, and both the forward and the backward propagating beams self-focus within a few seconds into a CP vector soliton of 20 μm FWHM, tightly overlapping (not shown). When the propagation distance is increased from 5 mm to 23 mm, for identical other conditions, the beams still self-focus approximately into solitons, but they do not overlap anymore [Fig. 2(a)]. At the exit face most of the beam intensity is expelled to a transversely shifted position (about 1 beam width), while a fraction of the beam remains guided by the other beam. At higher applied fields (stronger nonlinearity) the beams start to move. The motion is such that the exiting beam rotates about or rapidly passes through the input beam, or dances irregularly around. No such long-lasting temporal changes are observed in the copropagation geometry, and no transverse splitup transition of copropagating overlapping solitons has been reported, to the best of our knowledge [14]. All these dynamical phases can qualitatively be reproduced by numerical simulation (Fig. 3).

To understand the behavior of CP solitons we formulated a time-dependent model for the formation of self-trapped bidirectional waveguides [15]. It consists of wave equations in the paraxial approximation for the propagation of forward and backward beams, and a relaxation equation for the generation of space charge field in the PR crystal, in the isotropic approximation. We view CP solitons as self-trapped beams with internal modes, whose dynamics is caused by the changes in the space charge field. The model equations in the computational space are of the form:

$$i\partial_z F = -\Delta F + \Gamma E F, \qquad -i\partial_z B = -\Delta B + \Gamma E B, \quad (1)$$

$$\tau\partial_t E + E = -\frac{I}{1+I} \quad (2)$$

where Δ is the transverse Laplacian, $I = |F|^2 + |B|^2$ is the laser light intensity (in units of the background intensity), τ is the relaxation time of the crystal, which also depends on the total intensity, $\tau = \tau_0/(1+I)$, and Γ is the dimensionless coupling strength. Temporal derivatives are eliminated from Eq. (1), due to slow medium response [16]. To further simplify matters, we did not account for the temperature (diffusion) effects. In experiment, these effects were compensated by focusing the input B beam at the place of the exit and in the direction of the output F beam.

The propagation equations are solved numerically, concurrently with the temporal equations, in the manner described in Ref. [15]. Numerical treatment of CP beams is

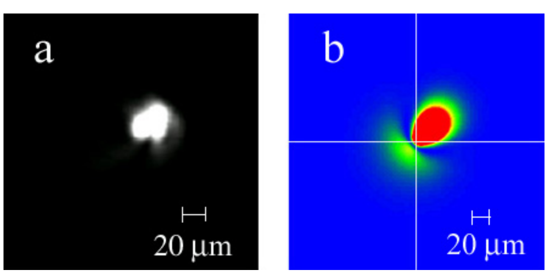

FIG. 2 (color online). CP soliton after a splitup transition: Forward propagating component in the steady state. (a) Exit face of the crystal, experimental. (b) The corresponding numerical simulation for $|F_0|^2 = |B_L|^2 = 0.5$, $\Gamma = 7.17$, and $L = 5.75L_D = 23$ mm.

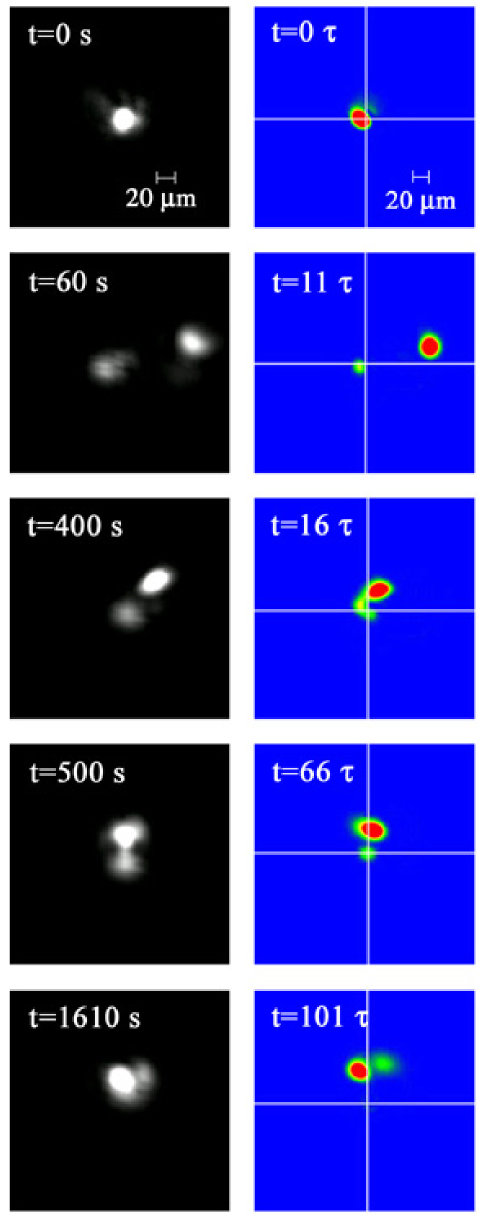

FIG. 3 (color online). Typical dynamic behavior of CP solitons in the unstable region. Left column is an experimental run, right column the corresponding numerical simulation. Parameters are as in Fig. 2, except for $|F_0|^2 = |B_L|^2 = 7$.

more complicated than the treatment of copropagating beams, owing to the essential difference between the two processes: copropagation is an initial-value problem, whereas counterpropagation is a two-point boundary-value problem. The presumed dynamics is such that the space charge field builds up towards the steady state, which depends on the light distribution, which in turn is enslaved to the change in the space charge field. The numerical procedure consists in solving Eq. (2) for the space charge field E in time, with the light fields obtained at every step as guided modes of the induced common waveguide [15]. The convergence in the temporal loop signifies that steady states are found, but it is not necessarily attained. In that case time-dependent, dynamical states are observed.

The results of numerical simulations are displayed in Figs. 2 and 3, together with the experimental results. In both experiment and simulations unstable regions are reached upon increasing the thickness of the crystal and the coupling strength. In numerics we also varied the intensity of laser light. Dynamical behavior in numerical simulations qualitatively follows that of the experimental runs. Typically output beam spots rotate about the input beam positions, or rapidly pass through them, until stable displaced equilibrium positions are found. In the case when no equilibrium is found (for larger ΓL) the output beams continue to dance about the input beams indefinitely. The first passage through the threshold is reminiscent of a Hopf bifurcation: a stable equilibrium becomes unstable and a limit cycle forms about. Previously attractive interaction between CP beams becomes repelling, and the beams rotate about each other.

It is difficult to explain this behavior theoretically. In the standard theory of modulational instabilities (MI) one follows the dynamics of weak perturbation to a broad wave and looks for instances of exponential growth of the perturbation. Such a growth promotes the amplification of sidebands and leads to the appearance of localized transverse structures. This approach is used much in the theory of transverse optical patterns [17]. Here however, the whole object—a CP soliton—undergoes a symmetry breaking transverse shift to a new position. In our earlier publication [18] we presented a simple theory of beam displacement that can account for such shifts. We attempt here to utilize the standard MI theory to obtain the threshold curve for the CP soliton splitup that will at least qualitatively agree with the experimental and numerical results. We suppose that above the critical wave vector k_c^2 the unstable ring in the transverse k space will focus to a spot, to which most of the energy (intensity) of the initial beam will be transferred. The assumption is that a localized peaked structure in the direct space will form a localized peaked structure in the inverse space, and that their dynamics, in both z and t, will be correlated. This expectation is based on the fact that the expectation value of the soliton position in the transverse plane and the corresponding soliton momentum form a conjugate pair of variables, so that the motion of soliton's "center of mass" is governed by Hamilton's equations [18,19].

One starts at the steady state plane-wave solution:

$$F_0(z) = F_0(0)e^{-i\Gamma E_0 z}, \qquad B_0(z) = B_0(L)e^{i\Gamma E_0(z-L)}, \quad (3)$$

where $E_0 = -I_0/(1 + I_0)$. It is clear that a plane wave is a poor approximation to the stable CP soliton; however, it is known [20] that the agreement with experiment can be improved by using initial beams of hyper-Gaussian profile. We are applying LSA to a low-aspect-ratio geometry, aware of its limited validity, in hopes of obtaining an estimate on the threshold location in the parameter space that will correlate with numerical results. The primary threshold is determined by the linear instability of steady state plane-wave field amplitudes $F_0(z)$ and $B_0(z)$, and the homogeneous part of the space charge field E_0. To perform LSA, a change of variables is made:

$$F = F_0(1 + f), \qquad B = B_0(1 + b), \qquad E = E_0(1 + e), \quad (4)$$

along with the change in the boundary conditions $f(0) = b(L) = 0$.

Neglecting higher harmonics and quadratic terms in the perturbations f, b, and e, and following the procedure described in Ref. [21], we obtain the threshold condition in a form:

$$2 + 2\cos\Psi_1\cos\Psi_2 + \left(\frac{\Psi_1}{\Psi_2} + \frac{\Psi_2}{\Psi_1}\right)\sin\Psi_1\sin\Psi_2 = 0 \quad (5)$$

where $\Psi_1 = k^2L$, $\Psi_2 = \sqrt{k^4L^2 - 4A\Gamma k^2L^2}$. We choose $|F_0|^2 = |B_L|^2$, so that $A = |F_0|^2/(1 + 2|F_0|^2)^2$. This equation has the same form as the threshold condition in Ref. [22], except that the form and the meaning of variables Ψ_1 and Ψ_2 is different.

It is difficult to compare experimental and numerical results with the threshold curves represented in Fig. 4, because for each value of A there are two values of $|F_0|^2$ (or $|B_L|^2$). For this reason we find it more convenient to plot the threshold intensity as a function of the square of the transverse wave vector (Fig. 5); for each pair of values

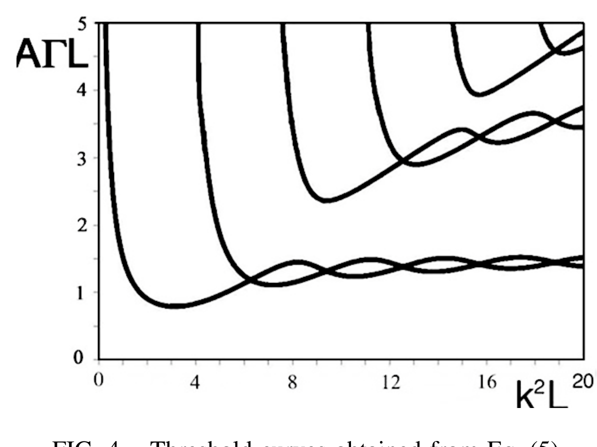

FIG. 4. Threshold curves obtained from Eq. (5).

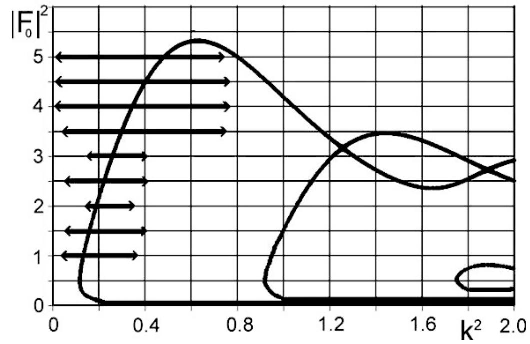

FIG. 5. Threshold intensity $|F_0|^2$ (or $|B_L|^2$) versus the square of transverse wave vector k^2, for $\Gamma = 4$ and $L = 5L_D$. Arrows cover the regions of jump in k^2 of the solitons in the inverse space, obtained numerically.

of Γ and L then one obtains different threshold curves. An analysis of Eq. (5) for the given Γ and L gives an extra condition:

$$k^2 < \Gamma/2, \tag{6}$$

which means that the critical k^2 is not arbitrary large, as it might seem from Fig. 4.

Also provided in Fig. 5 are the arrows which depict how much the CP solitons jump transversely in the k space in numerical simulations, after a splitup transition. The left end of an arrow points to the peak value of k^2 in the steady state; the right end points to the maximum value of the total transient change in k^2. This end evidently complies with the condition in Eq. (6). The end points are calculated by independent numerical runs of the full simulations. For the given control parameters ($\Gamma = 4$ and $L = 5L_D$) only single or double splitup transitions are observed. It is seen that the arrows provide a qualitative agreement with the form and the position of the lowest branch of the threshold curve, which signifies the first splitup transition. It is difficult to see higher order transitions, because of the intervening dynamical effects. When $\Gamma = 7.17$ and $L = 5.75L_D$, as in one of the experiments, a complicated dynamical behavior is observed, since it lies in the region of intensities where the threshold curves cross each other and where the influence of the saturable nonlinearity is the largest. Below and above this region the dynamics become simpler, and CP solitons cease to exist. These facts are confirmed experimentally: CP solitons can exist only in a certain window of beam intensities.

In conclusion, we have established the existence of 2D CP vector solitons in an SBN:60Ce PR crystal. We have displayed their varied dynamical behavior and carried out numerical simulations that confirm our experimental findings. We have performed LSA that predicted a threshold for the splitup instability of CP solitons, in qualitative agreement with numerical simulations.

Work at the Institute of Physics is supported by the Ministry of Science and Environment Protection, under the project no. OI 1475. Part of this work was supported by the Deutsche Forschungsgemeinschaft.

[1] *Spatial Solitons*, edited by S. Trillo and W. Torruellas (Springer, New York, 2001).
[2] For an overview see the Special Issue on solitons, edited by M. Segev [Opt. Photonics News **13**, 2 (2002)].
[3] M. Shih, M. Segev, and G. Salamo, Phys. Rev. Lett. **78**, 2551 (1997).
[4] M. Shih, M. Segev, Opt. Lett. **21**, 1538 (1996).
[5] A. A. Zozulya, D. Z. Anderson, A. V. Mamaev, and M. Saffman, Phys. Rev. A **57**, 522 (1998).
[6] M. Saffman, G. McCarthy, and W. Krolikowski, J. Opt. B **6**, S397 (2004).
[7] N. Fressengeas, J. Maufoy, and G. Kugel, Phys. Rev. E **54**, 6866 (1996).
[8] C. Denz *et al.*, Phys. Rev. E **60**, 6222 (1999).
[9] M. Haelterman, A. P. Sheppard, and A. W. Snyder, Opt. Commun. **103**, 145 (1993).
[10] O. Cohen, R. Uzdin, T. Carmon, J. W. Fleischer, M. Segev, and S. Odulov, Phys. Rev. Lett. **89**, 133901 (2002).
[11] O. Cohen, S. Lan, T. Carmon, J. A. Giordmaine, and M. Segev, Opt. Lett. **27**, 2013 (2002).
[12] C. Rotshield, O. Cohen, O. Mandela, T. Carmon, and M. Segev, J. Opt. Soc. Am. B **21**, 1354 (2004).
[13] M. Golubitsky, I. Stewart, and D. Schaeffer, *Singularities and Groups in Bifurcation Theory*, Applied Mathematical Sciences, 69 (Springer-Verlag, New York, 1988), Vol. II.
[14] Reference [5] reports transverse splitting of single solitons.
[15] M. Belić, Ph. Jander, A. Strinić, A. Desyatnikov, and C. Denz, Phys. Rev. E **68**, 025601 (2003).
[16] The full time-dependent nonlocal model might be treatable by the methods of center manifold reduction.
[17] Special Issue on Nonlinear structures in dissipative systems, edited by R. Friedrich, T. Kuhn, and S. J. Linz [Ann. Phys. (Leipzig) **13**, 7 (2004)].
[18] M. Belić, M. Petrović, D. Jović, A. Strinić, D. Arsenović, K. Motzek, F. Kaiser, Ph. Jander, C. Denz, M. Tlidi, and P. Mandel, Opt. Express **12**, 708 (2004).
[19] One can also decompose the soliton field in terms of Gauss-Hermite or Gauss-Laguerre basis functions in the direct and in the inverse space. Since these functions have the same form in both spaces (up to simple factors) the motion of soliton in the direct space will be correlated to the motion in the inverse space.
[20] O. Sandfuchs, F. Kaiser, and M. R. Belić, Phys. Rev. A **64**, 063809 (2001).
[21] M. Schwab, C. Denz, and M. Saffman, J. Opt. Soc. Am. B **18**, 628 (2001).
[22] J. B. Geddes, R. A. Indik, J. V. Moloney, and W. J. Firth, Phys. Rev. A **50**, 3471 (1994).